Received: 11 October 2022 | Accepted: 6 December 2022

DOI: 10.1111/gcb.16583

RESEARCH ARTICLE

Global Change Biology WILEY

Rapid and large changes in coastal wetland structure in China's four major river deltas

Xinxin Wang[1] | **Xiangming Xiao**[2] | **Xi Zhang**[1] | **Jihua Wu**[3] | **Bo Li**[4]

[1]Ministry of Education Key Laboratory for Biodiversity Science and Ecological Engineering, National Observations and Research Station for Wetland Ecosystems of the Yangtze Estuary, Institute of Biodiversity Science and Institute of Eco-Chongming, School of Life Sciences, Fudan University, Shanghai, China

[2]Department of Microbiology and Plant Biology, Center for Earth Observation and Modeling, University of Oklahoma, Norman, Oklahoma, USA

[3]State Key Laboratory of Grassland Agro-Ecosystems, and College of Ecology, Lanzhou University, Lanzhou, China

[4]Yunnan Key Laboratory of Plant Reproductive Adaptation and Evolutionary Ecology and Centre for Invasion Biology, Institute of Biodiversity, School of Ecology and Environmental Science, Yunnan University, Kunming, China

Correspondence

Xiangming Xiao, Department of Microbiology and Plant Biology, Center for Earth Observation and Modeling, University of Oklahoma, Norman, OK 73019, USA.
Email: xiangming.xiao@ou.edu

Bo Li, Yunnan Key Laboratory of Plant Reproductive Adaptation and Evolutionary Ecology and Centre for Invasion Biology, Institute of Biodiversity, School of Ecology and Environmental Science, Yunnan University, Kunming, Yunnan 650504, China.
Email: bool@ynu.edu.cn

Funding information

National Key Research and Development Program of China, Grant/Award Number: 2022YFC2601100; Natural Science Foundation of China, Grant/Award Number: 32030067, 42201341 and 41630528; China Postdoctoral Science Foundation, Grant/Award Number: 2021TQ0072 and 2021M700835; U.S. National Science Foundation, Grant/Award Number: 1911955 and 2200310

Abstract

Coastal wetlands provide essential ecosystem goods and services but are extremely vulnerable to sea-level rise, extreme climate, and human activities, especially the coastal wetlands in large river deltas, which are regarded as "natural recorders" of changes in estuarine environments. In addition to the area (loss or gain) and quality (degradation or improvement) of coastal wetlands, the information on coastal wetland structure (e.g., patch size and number) are also major metrics for coastal restoration and biodiversity protection, but remain very limited in China's four major river deltas. In this study, we quantified the spatial–temporal dynamics of total area (TA) and patch number (PN) of coastal wetlands with different sizes in the four deltas and the protected areas (PAs) and assessed the effects of major driving factors during 1984–2020. We also investigated the effectiveness of PAs through the comparison of TA and PN of coastal wetlands before and after the years in which PAs were listed as Ramsar Sites. We found both TA and PN experienced substantial losses in the Liaohe River Delta and Yellow River Delta but recent recoveries in the Yangtze River Delta. The coastal wetlands had a relatively stable and variable trend in TA but had a continually increasing trend in PN in the Pearl River Delta. Furthermore, reduced coastal reclamation, ecological restoration projects, and rapid expansion of invasive plants had great impacts on the coastal wetland structure in various ways. We also found that PAs were effective in halting the decreasing trends in coastal wetland areas and slowing the expansion of reclamation, but the success of PAs is being counteracted by soaring exotic plant invasions. Our findings provide vital information for the government and the public to address increasing challenges of coastal restoration, management, and sustainability in large river deltas.

KEYWORDS

China's major river deltas, coastal wetland structure, patch number, patch size, plant invasion, protected area, *Spartina alterniflora*

1 | INTRODUCTION

Coastal wetlands interact with both ocean and terrestrial ecosystems and provide crucial ecosystem services for human beings and wildlife (Ma et al., 2014; Murray et al., 2022; Wang et al., 2021). However, because of climate change (e.g., sea level rise, storms) and intensified anthropogenic activities (e.g., land reclamation, eutrophication, invasive species), coastal wetlands have been substantially degraded or disappeared over the last few decades (He & Silliman, 2019; Jia et al., 2021; Murray et al., 2022). In particular, the coastal wetlands in large river deltas, which provide key habitats for migratory birds, fish, and other biological resources, are extremely vulnerable to natural or anthropogenic disturbances (Ma et al., 2019), and are regarded as "natural recorders" of changes in estuarine environments (Bianchi & Allison, 2009). For example, mangrove forest cover in the Ayeyarwady delta of Myanmar declined by 64.2% at an average rate of 51 km^2 $year^{-1}$ (3.1%) during 1978–2011 (Richards & Friess, 2016; Webb et al., 2014); coastal wetlands in the Mississippi River delta have experienced considerable losses of 5197 km^2 since the 1930s (Ryu et al., 2021); significant losses of coastal wetlands during 1984–2018 (slope = 10.0 ± 5.29 km^2 $year^{-1}$) were also found in the Yellow River Delta (YRD) of China (Wang et al., 2021).

Intensified natural or anthropogenic disturbances not only cause the losses of coastal wetlands but also exacerbate the substantial changes in their structures (e.g., patch size and number), which have substantial effects on coastal restoration and biodiversity protection (Haddad et al., 2015; Lindenmayer, 2019; Timmers et al., 2022; Wilson et al., 2016). For example, integrated coastal wetlands with larger patch sizes usually have better ecological functions, such as water purification, carbon sequestration, and sediment deposition (Barbier et al., 2011). However, tidal creeks are often introduced in ecological restoration projects to divide large coastal wetland patches into some isolated and small ones for higher hydrodynamic and biological connections, which could provide more habitats for nekton and shorebirds (Xie et al., 2020). Thus, quantitative evaluation of the spatial–temporal characteristics of coastal wetland structure is of great significance to regional protection and management and biodiversity protection and is crucial for achieving coordinated socioeconomic development and ecosystem protection.

In China, more than 41% of the population, 70% of large and medium-sized cities, and two-thirds of the Gross Domestic Product are settled in the four major river deltas: Liaohe River Delta (LRD), YRD, Yangtze River Delta (YtRD), and Pearl River Delta (PRD) (Ma et al., 2019). The coastal wetlands in these four deltas play significant roles in biodiversity protection, for example, they provide important habitats for 50 million migratory birds in the East Asian-Australasian Flyway (EAAF) (Croxall et al., 2012; Ren et al., 2021; Yang et al., 2017). However, coastal wetlands in China's major river deltas are under intense pressure from reclamation (Wang et al., 2021, 2022), plant invasions (Ning et al., 2019, 2021; Wang et al., 2022), sea level rise (Ma et al., 2019), and reduced sediment loads from the rivers (Wang, Xiao, Zou, Chen, et al., 2020), contributing to the great changes in coastal wetland structure and posing substantial threats to the ecological security of coastal deltas (Ning et al., 2020). Several remote-sensing studies have reported information on coastal wetland structure in China's major river deltas in specific year(s), such as the LRD in 1980, 1990, 2000, 2010, and 2020 (Tan et al., 2022), the YRD in 2000, 2005 and 2010 (Liu et al., 2014), and the PRD in 1980, 1990, 2000, 2010, and 2010 (Zhou et al., 2019). However, these studies did not document annual and multi-decadal changes in patch size and number. Furthermore, the impacts of plant invasions, dam construction, and ecological restoration projects on the coastal wetland structure, and the effectiveness of major protected areas (PAs) in protecting coastal wetlands are still yet not fully explored in China's major river deltas.

Here, we generated the annual coastal wetland maps (including tidal flats, saltmarshes, and mangrove forests) in China's four major river deltas during 1984–2020 using time series Landsat satellite images and the pixel- and phenology-based mapping tool (Wang et al., 2021). Second, we analyzed the dynamics of patch area and number of coastal wetlands with different sizes in four deltas and assessed the effectiveness of PAs. Third, we explored the impacts of reclamation, plant invasion (*Spartina alterniflora*, hereafter, *Spartina*), sediment discharges, and ecological restoration projects on the coastal wetland structure, and discussed the implications for the protection, restoration, and sustainability of coastal wetlands in large river deltas.

2 | MATERIALS AND METHODS

2.1 | Study area

In this study, we focused on the dynamics of coastal wetland structure in China's four major river deltas (the LRD, YRD, YtRD, and PRD), and all of which were formed by sediment discharge from large rivers (Figure 1). The LRD is situated in Liaoning Province of Northeast China and comprises the largest reed fields in the world (Ma et al., 2019). The YRD, situated in Shandong Province, has the largest amount of mud and sand, and is the largest river delta in China (Wang et al., 2021), providing important habitats for native wildlife and migratory birds in the EAAF (Ren et al., 2021). The YtRD, which includes Shanghai municipality and the southern coastal zone of Jiangsu Province, is the largest and key stopover site for migratory birds in the EAAF (Zhang, Xiao, et al., 2020). The PRD, located in the south of Guangdong Province, is one of the most highly urbanized regions and most developed regions in the world (Ma et al., 2019).

Four key PAs have been established in China's four deltas (Table S1). In 1988, Shuangtaihekou National Nature Reserves (NNRs) in the LRD, whose name was changed to Liaoning Liaohe Estuary NNR in 2015 (LHPA), was established to conserve the coastal wetlands with an area of ~1271.52 km^2, which was listed as a Ramsar site in 2005 (Ma et al., 2019; Ren et al., 2021). YRD NNR (YRPA) was established in 1992 and was listed as a Ramsar site in 2013. In the YtRD, the Shanghai Chongming Dongtan Bird NNR (CMPA) and the Shanghai Jiuduansha Wetland National Nature Reserve of the YtRD

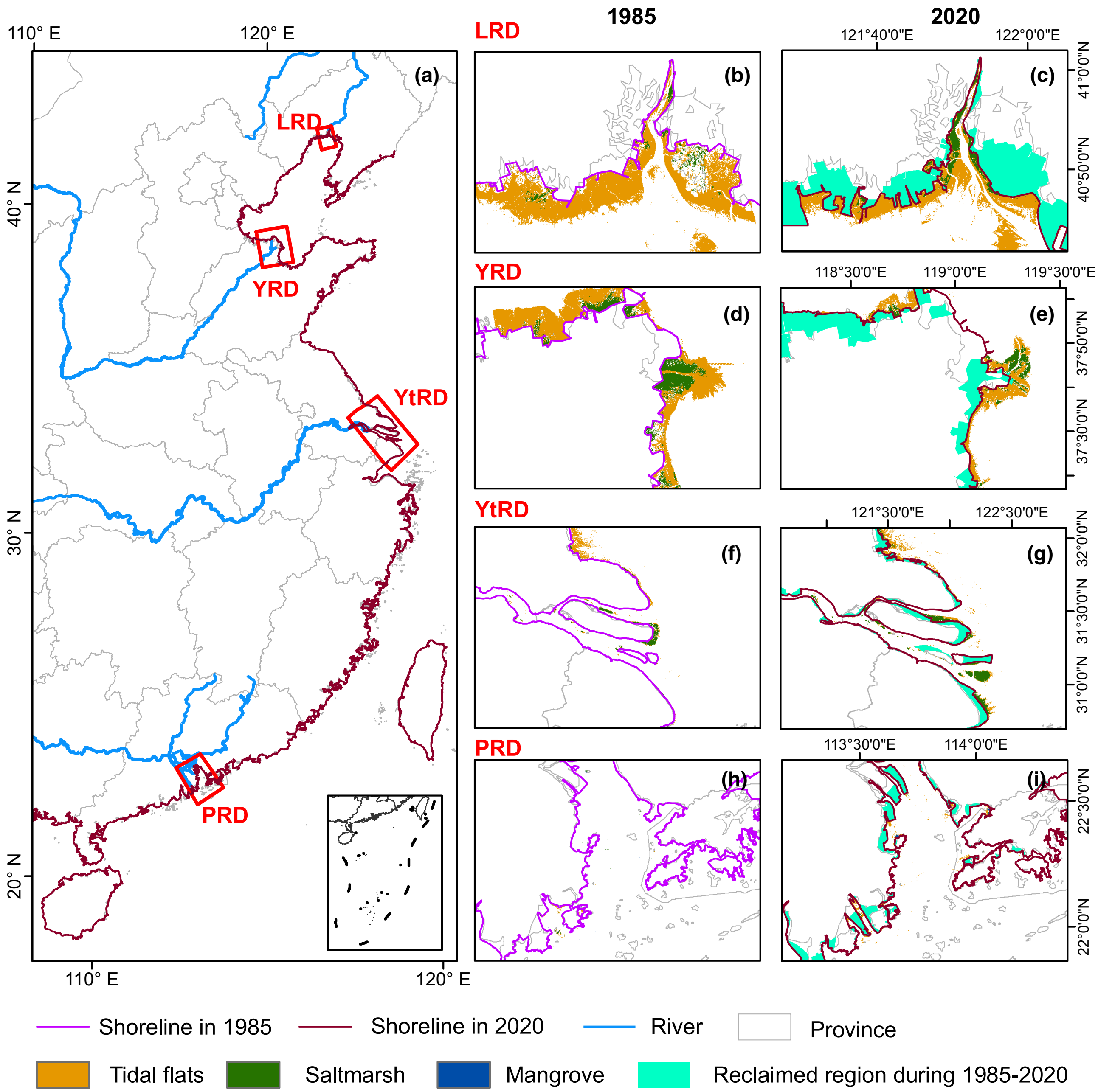

FIGURE 1 Study area. (a) Locations of four major rivers, Liaohe River Delta (LRD), Yellow River Delta (YRD), Yangtze River Delta (YtRD), Pearl River Delta (PRD), and shoreline in 2020. (b, c) Coastal wetlands of the LRD in 1985 and 2020. (d, e) Coastal wetlands of the YRD in 1985 and 2020. (f, g) Coastal wetlands of the YtRD in 1985 and 2020. (h, i) Coastal wetlands of the PRD in 1985 and 2020. The reclaimed regions during 1985–2020 are also shown in subfigure (c, e, g, and i). Map lines delineate study areas and do not necessarily depict accepted national boundaries.

(JDSPA) were established in 2005, of which the CMPA was listed as a Ramsar site in 2002 (Table S1).

2.2 | Data

2.2.1 | Landsat data

We acquired all the available time series Landsat Collection 2 Level-2 (TM/ETM/OLI) surface reflectance (SR) images in China's four major river deltas from January 1, 1984, to December 31, 2020, from the Google Earth Engine (GEE) cloud-processing platform. Landsat acquires images at 16-day revisit cycle and 30-m spatial resolution. All poor-quality observations in Landsat collections, including clouds and cloud shadows, were identified and removed through the quality assessment band (QA_PIXEL). As the limited good-quality observations of Landsat data in these deltas before 1990 (Figure S1), we generated the coastal wetland maps within each 3-year time period during 1984–1989; for example, we generated the coastal wetland maps in 1985 using the time series Landsat data during 1984–1986, and generated the maps in

1988 using the Landsat data during 1987–1989. This approach enabled us to have enough numbers of good-quality observations in each 3-year period to generate the final maps (Wang et al., 2021).

The Enhanced Vegetation Index (EVI), Normalized Difference Vegetation Index (NDVI), Land Surface Water Index (LSWI), and the Modified Normalized Difference Water Index (mNDWI) were used to identify coastal wetlands in this study, which were calculated using the equations below:

$$\mathrm{NDVI} = \frac{\rho_{\mathrm{nir}} - \rho_{\mathrm{red}}}{\rho_{\mathrm{nir}} + \rho_{\mathrm{red}}} \tag{1}$$

$$\mathrm{EVI} = 2.5 \times \frac{\rho_{\mathrm{nir}} - \rho_{\mathrm{red}}}{\rho_{\mathrm{nir}} + 6 \times \rho_{\mathrm{red}} - 7.5 \times \rho_{\mathrm{blue}} + 1} \tag{2}$$

$$\mathrm{LSWI} = \frac{\rho_{\mathrm{nir}} - \rho_{\mathrm{swir}}}{\rho_{\mathrm{green}} + \rho_{\mathrm{swir}}} \tag{3}$$

$$\mathrm{mNDWI} = \frac{\rho_{\mathrm{green}} - \rho_{\mathrm{swir}}}{\rho_{\mathrm{green}} + \rho_{\mathrm{swir}}} \tag{4}$$

where ρ_{blue}, ρ_{green}, ρ_{red}, ρ_{nir}, and ρ_{swir} are the SR values of blue, green, red, near-infrared, and shortwave infrared bands in Landsat images.

2.2.2 | Geospatial datasets of the driving factors

The driving factors were grouped into three categories: (1) land-use and land-cover changes, including reclamation area and invasive *Spartina* area as coastal reclamation and plant invasions are regarded as the most important factors driving the rapid changes of coastal wetlands (Ma et al., 2014; Ning et al., 2019, 2021; Wang et al., 2022); (2) sea level rise; (3) sediment load, which directly affects the deposition rates of mud and sand in river deltas (Wang, Xiao, Zou, Hou, et al., 2020) (Figure S2).

1. *Areas of Spartina and reclamation*. Annual areas of invasive *Spartina* and reclamation in four major river deltas during 1984–2020 were calculated using the algorithms in Sections 2.3.2 and 2.3.3.
2. *Sea level data*. Annual sea level anomaly data during 1984–2020 in China were collected from the China Sea Level Bulletin (available at http://www.mnr.gov.cn/sj/sjfw/hy/gbgg/zghpmgb/).
3. *Sediment load data*. We collected annual sediment load data in the four deltas for the period 1984–2020 from the annual Chinese River Sediment Bulletin (available at http://www.irtces.org/nszx/cbw/hlnsgb/A550406index_1.htm).

2.3 | Methods

The workflow of this study comprised major four steps: (1) identification of surface water body, green vegetation, and mangrove forest for individual observations and pixels; (2) frequency estimates of surface water body, green vegetation, and mangrove canopy in a year for individual pixels; (3) classification of coastal wetlands (including tidal flats, saltmarshes, and mangrove forests) for individual pixels; and (4) generation of annual maps of coastal wetlands in four deltas during 1984–2020 (Figure S3).

2.3.1 | Generation of annual maps of mangrove forests, saltmarshes, and tidal flats

1. Identification of surface water body, green vegetation, and mangrove forest for individual observations.

We combined the mNDWI, NDVI, and EVI indices to identify surface water bodies ((mNDWI > EVI or mNDWI > EVI) and (EVI < 0.1)), and this algorithm could reduce the commission errors induced by green vegetation (Zou et al., 2018). We also combined NDVI, EVI, and LSWI to map green vegetation (EVI ≥ 0.1 and NDVI ≥ 0.2 and LSWI > 0), which has already been used to identify tidal vegetation (Wang et al., 2021) and coastal *Spartina* saltmarshes (Zhang, Xiao, et al., 2020). In addition, we used (NDVI > 0.3 and LSWI > 0.3) as criteria to identify mangrove forests (Chen et al., 2017).

2. Frequency estimates of surface water bodies, green vegetation, and mangrove forests per pixel in a year.

A frequency-based approach was used in this study to maximize the benefits of time series Landsat images and reduce the errors induced by poor-quality observations, periodical tides, and phenological information of tidal vegetation (Wang, Xiao, Zou, Hou, et al., 2020). For example, the surface water frequency (F_{SW}) of a pixel in a year was calculated using Equation (5).

$$F_{\mathrm{sw}} = \frac{N_{\mathrm{SW}}}{N_{\mathrm{Good}}} \tag{5}$$

where F_{sw} is the frequency of open surface water bodies in a year, ranging from 0 and 1 (100%) among all the good-quality observations; N_{SW} is the number of surface water body observations in a year; and N_{Good} is the number of good-quality observations in a year.

Similarly, we calculated the green vegetation frequency (F_{GV}) and mangrove forest frequency (F_{MF}) using Equations (6) and (7).

$$F_{\mathrm{GV}} = \frac{N_{\mathrm{GV}}}{N_{\mathrm{Good}}} \tag{6}$$

$$F_{\mathrm{MF}} = \frac{N_{\mathrm{MF}}}{N_{\mathrm{Good}}} \tag{7}$$

3. Algorithms for classifying coastal wetlands per pixel.

In our study, coastal wetlands were divided into two subgroups (tidal vegetation and unvegetated tidal flats), with tidal vegetation being further divided into coastal saltmarshes and mangrove forests

(Murray et al., 2022; Wang et al., 2021). Tidal flats and tidal vegetation were first identified by using different thresholds of F_{SW} and F_{GV} (Equations 8 and 9). After that, mangrove forests were separated within tidal vegetation using Equations (10)–(12) (Chen et al., 2017). Finally, the rest of tidal vegetation was regarded as saltmarshes (Wang et al., 2021).

$$\text{Tidal flat} = F_{GV} < 0.15 \text{ and } 0.05 < F_{SW} < 0.95 \tag{8}$$

$$\text{Tidal vegetation} = F_{GV} \geq 0.15 \text{ and } F_{SW} \leq 0.2 \tag{9}$$

$$F_{SW}(x) > \begin{cases} 70 & x < 0.28 \\ -155.81x + 114.01 & 0.28 \leq x < 0.73 \\ 0 & x \geq 0.73 \end{cases} \tag{10}$$

$$F_{GV}(x) > \begin{cases} 20 & x < 0.25 \\ 211.47x - 33.46 & 0.25 \leq x < 0.54 \\ 80 & x \geq 0.54 \end{cases} \tag{11}$$

$$F_{MF}(x) > \begin{cases} 10 & x < 0.28 \\ 193.85x - 43.78 & 0.28 \leq x < 0.59 \\ 70 & x \geq 0.59 \end{cases} \tag{12}$$

where F_{SW}, F_{GV}, and F_{MF} are surface water frequency, green vegetation frequency, and mangrove forest canopy frequency calculated in a year; and x is annual mean NDVI in a year.

4. Generation of annual maps of coastal wetlands in four deltas during 1984–2020.

We used the visual image interpretation approach to delineate the man-made shorelines (e.g., aquaculture ponds, artificial engineering, artificial levee for reclamation and roads) to separate the natural coastal wetlands from other land cover types through integrating very high spatial resolution images of Google Earth and Landsat RGB images in each year during 1984–2020 (Chen et al., 2019). Based on these man-made shorelines, a 50-km buffer in marine environments was created as the potential natural coastal zone (Wang et al., 2021).

Within the potential coastal zone, we identified the type for each pixel (tidal flats, saltmarshes, and mangrove forests) according to Equations (8)–(12). Furthermore, the rules DEM <5 m and slope <5° were used as a supplementary criterion to limit the boundary of coastal wetlands (Chen et al., 2017). Finally, all the pixels with good-quality observations within potential coastal wetland zone were processed using the same mapping algorithms, and the annual coastal wetland maps of China's four major river deltas during 1984–2020 were generated in the GEE platform (Figure S4).

2.3.2 | Algorithm for identifying invasive *Spartina* saltmarshes

In this study, a phenology-based algorithm developed by Zhang, Xiao, et al. (2020) was used to identify the invasive *Spartina* saltmarshes. They investigated the phenology of *Spartina*, *Phragmites*, and *Scirpus* saltmarshes based on the vegetation indices acquired from time series Landsat data, and found that *Spartina* saltmarshes did not green up in April–May and stayed still green in December–January, which differed from the phenology of *Phragmites* and *Scirpus* saltmarshes. Therefore, the algorithm for identifying *Spartina* saltmarshes was shown in Equation (13).

$$Spartina = \text{LSWI}_{\text{mean(April–May)}} \leq 0 \cap F_{\text{GV(December–January)}} > 0 \tag{13}$$

where $\text{LSWI}_{\text{mean(April–May)}}$ is the mean value of LSWI during April–May, and $F_{\text{GV(December–January)}}$ is the green vegetation frequency during December–January. Therefore, we finally generated the annual maps and calculated annual *Spartina* areas during 1984–2020 in China's four major river deltas (Figures S5 and S6a–c).

2.3.3 | Calculation of reclaimed areas

Based on the 50-km buffer zone in marine environments created in Section 2.3.1, we generated the reclamation zone (RZ_y) using the buffer zone in a year (BZ_y) and the buffer zone in the previous year (BZ_{y-1}) (Equation 14). After that, we calculated the annual reclaimed area during 1988–2020 in China's four major river deltas (Figures S6d–g and S7).

$$RZ_y = BZ_y - BZ_{y-1} \tag{14}$$

where y is the year from 1988 to 2020.

2.3.4 | Geospatial and statistical analyses

We generated the annual vector maps of coastal wetlands and *Spartina* saltmarshes based on their raster maps using the "RasterToPolygon_conversion" algorithm in python, then reprojected them to the Krasovsky_1940_Albers equal-area conic projection. We then counted the patch numbers (PNs) of coastal wetlands and *Spartina* saltmarshes and calculated the total areas (TAs) of coastal wetlands, *Spartina* saltmarshes, and reclamation zone within each delta and PA. Furthermore, we calculated the patch density (PD) as the ratio of PN to TA. The interannual variations and trends in TA, PN, and PD of coastal wetlands during 1984–2020 at different spatial scales were calculated and analyzed through linear regression models with a t-test at the 5% significance level. Additionally, we also explored the relationship of tidal vegetation and tidal flat areas with other driving factors using simple and multiple linear regression models in R code (R Core Team, 2021).

3 | RESULTS

3.1 | Coastal wetland areas in the four deltas

In 2020, the coastal wetland area was largest in the YtRD (922.05 km^2), followed by the YRD (456.80 km^2), LRD (181.25 km^2), and PRD (114.64 km^2; Figure S8). During 1984–2020, the coastal wetland areas in the LRD and YRD showed significantly decreasing trends with rates of 1.61 km^2/year ($p < .01$) and 17.67 km^2/year ($p < .001$), respectively (Figure 2a,b). The coastal wetland area in the YtRD had high variations during 1984–2020, but it started to recover after 2012 (slope = 37.95 km^2/year, $p < .01$) whereas the PRD had a stable trend in the coastal wetland area (Figure 2c,d). The interannual changes in tidal vegetation areas had divergent trends among the four deltas during 1984–2020 (Figure 3). It had four phases over years in the LRD: (1) a relatively stable but variable phase during 1984–1998; (2) a slowly declining phase in 1999–2005 (−2.0 km^2/year, $p < .01$); (3) a rapidly increasing phase in 2006–2014 (3.4 km^2/year, $p < .001$); and (4) a rapid decline phase in 2015–2020 (−3.9 km^2/year, $p = .05$). However, it had only two phases in the YRD: (1) a rapidly decreasing phase from 1984 to 2000 (−10.5 km^2/year, $p < .01$) and (2) a relatively stable phase in 2000s and 2020s. The tidal vegetation area in the YtRD had three phases: (1) a relatively stable phase during 1984–2006; (2) a small area but stable phase during 2007–2012; and (3) a rapidly increasing phase during 2012–2020 (19.3 km^2/year, $p < .001$). It increased over years during 1984–2016 (0.4 km^2/year, $p < .001$) but decreased moderately after 2017 in the PRD.

The interannual changes of the tidal flat area also varied among the four deltas (Figure 3). It had large variations during 1984–2005 in the LRD, and then substantially lost during 2006–2020 (−3.7 km^2/year, $p < .01$). Similarly, the YRD also had two phases in its tidal flat areas: (1) a relatively stable phase during 1984–2005 and (2) a large loss phase during 2006–2020 (−24.7 km^2/year, $p < .001$). The tidal flat areas in the YtRD had large interannual variation during 1984–2020 with multiple phases, including the declining phase during 1984–1993, the increasing phase during 1994–1999, the declining phase during 2000–2012, and the increasing phase during 2014–2020. However, the tidal flat area in the PRD had two phases: (1) a relatively stable phase during 1984–2012 and (2) a large gain phase during 2013–2020 (5.5 km^2/year, $p < .05$).

3.2 | Coastal wetland areas with different sizes

We qualified the TA dynamics of coastal wetlands with different sizes (area <1 km^2 and area ≥1 km^2) in the four river deltas (Figure 4).

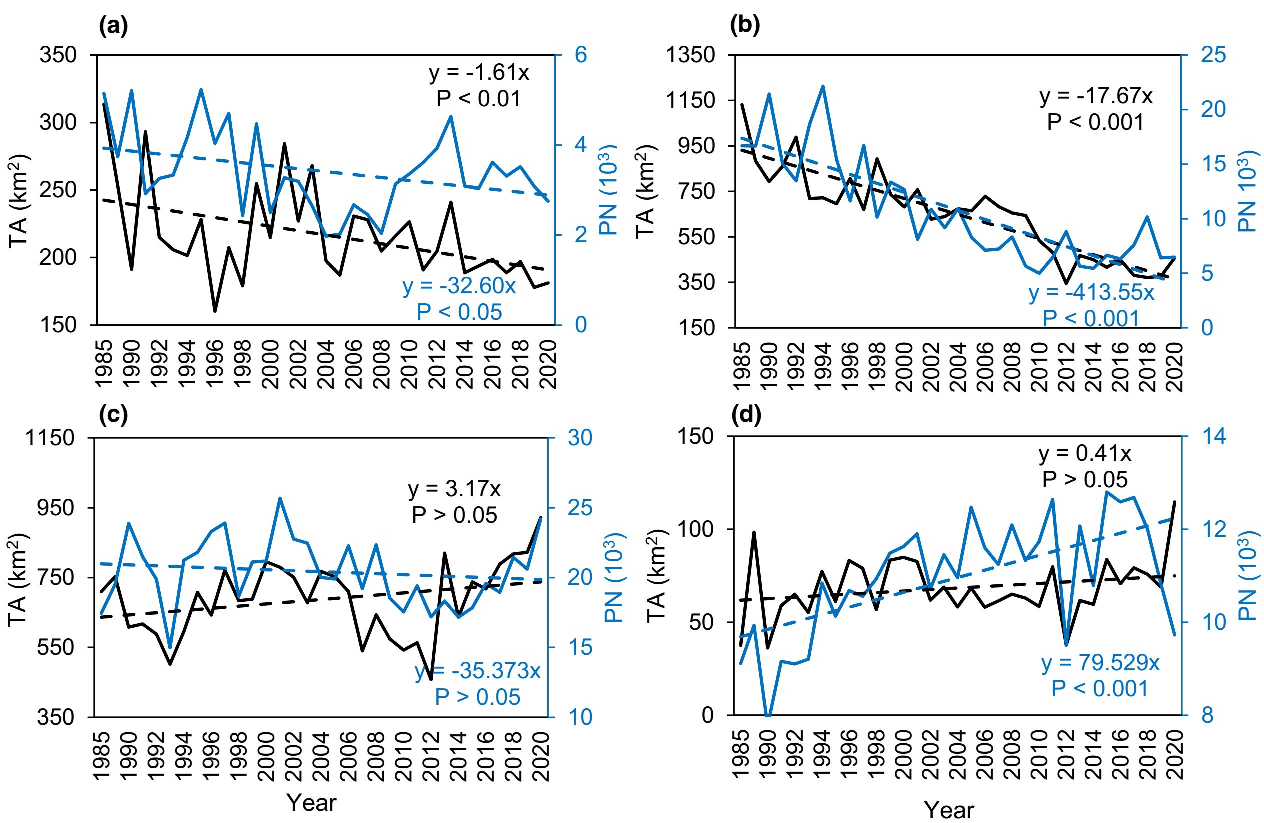

FIGURE 2 Total areas (TAs) and patch numbers (PNs) of coastal wetlands in China's four major river deltas during 1984–2020. (a) Liaohe River Delta (LRD). (b) Yellow River Delta (YRD). (c) Yangtze River Delta (YtRD). (d) Pearl River Delta (PRD).

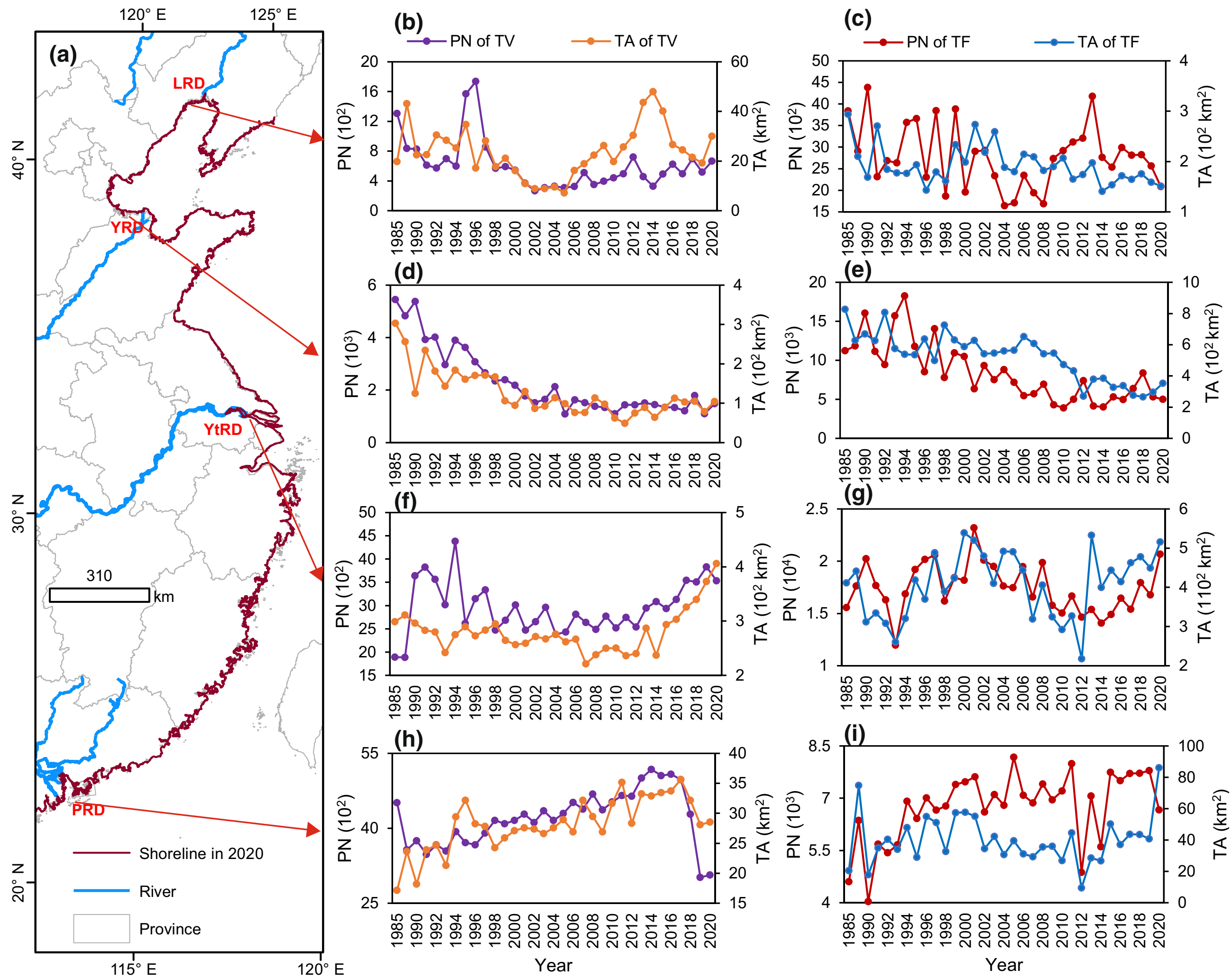

FIGURE 3 Total areas (TAs) and patch numbers (PNs) of tidal vegetation (TV) and tidal flats (TF) in China's four major river deltas during 1984–2020. (a) Spatial distribution of four deltas. (b, c) Liaohe River Delta (LRD). (d, e) Yellow River Delta (YRD). (f, g) Yangtze River Delta (YtRD). (h, i) Pearl River Delta (PRD).

As the TA of large patches accounted for a very large proportion of the TAs of coastal wetlands (Figure S8), the TA dynamics of large coastal wetland patches matched well with those of total coastal wetlands in four deltas. However, the small coastal wetland patches usually had different TA dynamics from those of large patches. The TA of small saltmarsh patches in the LRD had only three phases over years: (1) a relatively stable but variable phase during 1984–1997; (2) a rapidly declining phase in 1999–2004; and (3) a continually increasing phase in 2005–2020. However, it had four phases in the YtRD: (1) a stable phase during 1984–2005; (2) a sharply decreasing phase during 2006–2009; (3) a rapidly increasing phase during 2009–2013; and (4) a stable phase after 2013 (Figure 4d). The TA of small tidal vegetation in the PRD had similar dynamics to that of large patches before 2017, and it decreased substantially but the TA of large patches continually increased after 2017. The TA of small tidal flat patches in the LRD had two obvious phases over years: (1) a stable but variable phase between 1984 and 2000; and (2) a substantially decreasing phase during 2001–2020. In other three deltas, the TA of small tidal flat patches had similar dynamics to that of large patches although the TA of large patches had more outliers.

3.3 | PNs of coastal wetlands in the four major river deltas

We used the PN and PD for the analysis of PN dynamics of coastal wetlands. The PN in the four major deltas in 2020 had similar patterns with those of TA (Figure S8). The YtRD had the largest PN of coastal wetlands (24,193) in 2020, followed by the PRD (9729), YRD (6475), and LRD (2753), resulting in the largest PD of coastal wetlands in the PRD and their sparser distribution than other deltas (Figure S9). Although the PN of large patches of coastal wetlands was much smaller than that of small patches, their areas accounted for very large proportions of the TAs of coastal

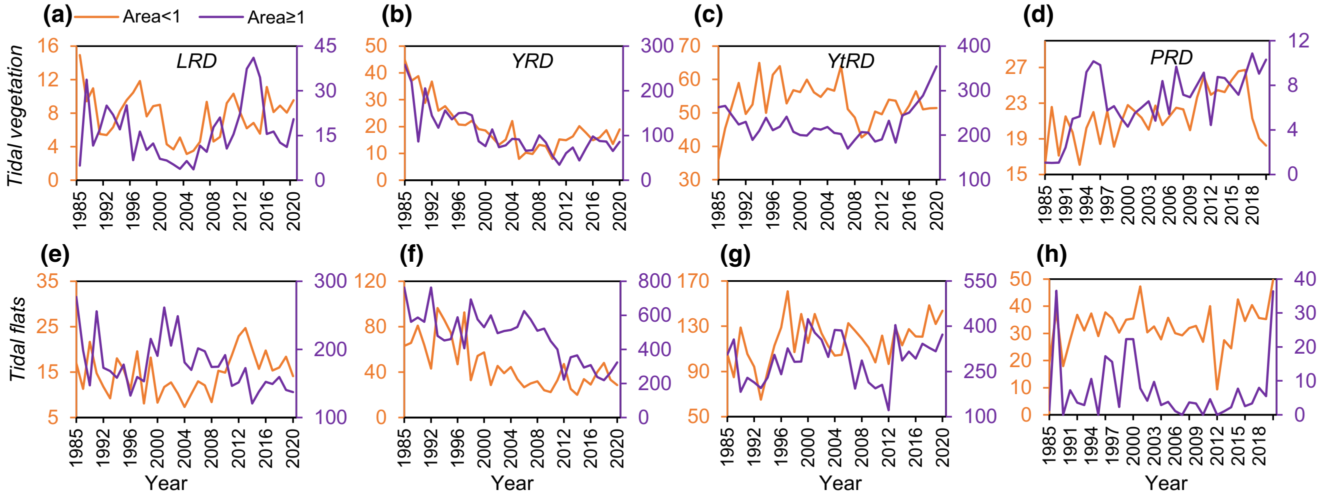

FIGURE 4 Total areas (TAs, km^2) of tidal vegetation and tidal flats with different sizes (area < 1 and area ≥1) in China's four major river deltas during 1984–2020. (a–d) TA of tidal vegetation with different sizes in four deltas. (e–h) TA of tidal flats with different sizes in four deltas.

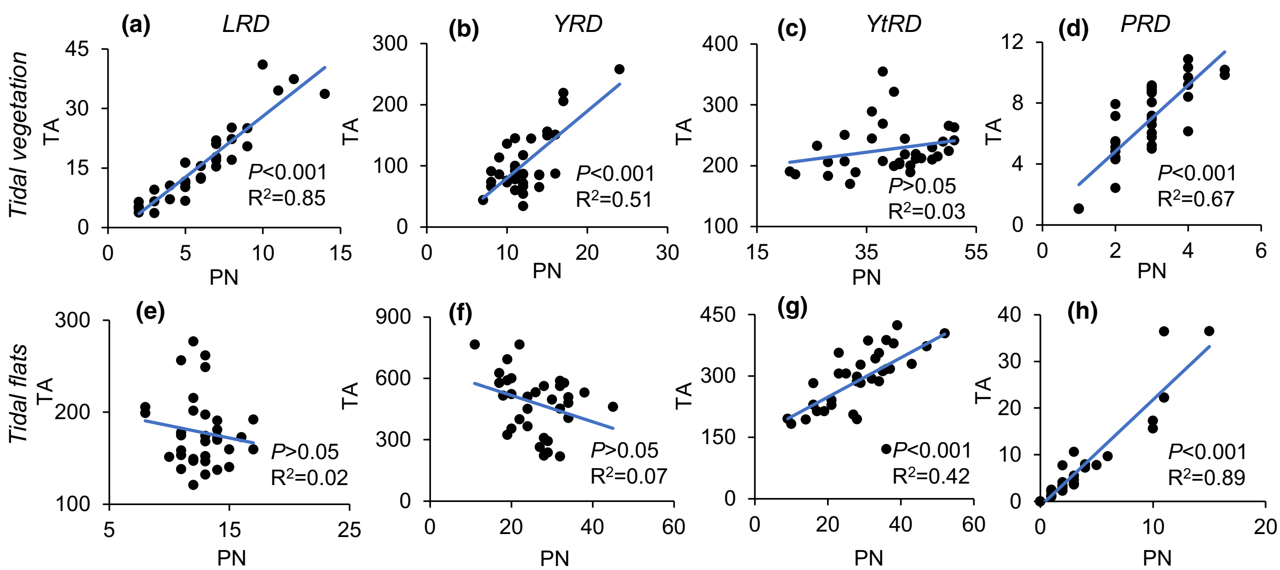

FIGURE 5 Relationships between patch number (PN) and total area (TA, km^2) of large tidal vegetation (TV) and tidal flat (TF) patches in China's four major river deltas during 1984–2020. (a–d) Relationships of tidal vegetation in four deltas. (e–h) Relationships of tidal flats in four deltas.

wetlands. During 1984–2020, the PNs of coastal wetlands in the LRD and YRD showed significantly decreasing trends with rates of 32.60 km^2/year ($p < .05$) and 413.55 km^2/year ($p < .001$), respectively, but it recently started to recover with large variation in the LRD after 2004 and showed a stable trend in the YRD after 2012 (Figure 2a,b). The PN of coastal wetlands in the YtRD had high variations during 1984–2020, but it also started to recover after 2012 (37.95 km^2/year, $p < .01$), which matched well with the trend of its areas (Figure 2c). The PRD showed a continually increasing trend in the PN of coastal wetlands during 1984–2020 ($p < .001$; Figure 2d).

The PN dynamics of tidal vegetation in the four deltas also matched well with the TA dynamics (Figure 3), although the PN trend of the LRD during 2004–2020 was much smoother than its TA trends. However, the PN of large tidal vegetation did not always change simultaneously with its TA (Figure S10). We found significant relationships in the LRD, YRD, PRD and non-positive relationship in the YtRD between PN and TA of large tidal vegetation patches (Figure 5), demonstrating the intensified anthropological interventions with tidal vegetation in the YtRD. The PN of tidal flats changed simultaneously with their TA in the YRD, YtRD, and PRD, nevertheless, the PN in the LRD experienced a substantially increasing trend while their TA experienced a significantly decreasing trend during 2004–2020. Furthermore, non-negative relationships in the LRD and YRD between PN and TA of large tidal flat patches also indicated their asynchronous changes.

3.4 | Coastal wetlands in the protected areas

We analyzed the dynamics of TA and PN of coastal wetlands within the PAs before and after the years in which PAs were listed as Ramsar Sites (Ramsar year) and assessed the effectiveness of PAs for protecting coastal wetlands (Figure 6). The TA and PN of tidal vegetation in the Liaoning Liaohe Estuary NNR (LHPA) experienced a substantial decrease with large variation before 2005 ($p<.01$), indicating the perilous state of coastal wetlands before the Ramsar year. After 2005, the TA had two noticeable phases: (1) a rapid recovery phase during 2005–2014 (slope = 3.95 km^2/year, $p<.001$); and (2) a rapidly decreasing phase during 2015–2020 (slope = −3.78 km^2/year, $p>.05$). However, the PN of tidal vegetation showed a significantly increasing trend (slope = 12.65/year, $p<.05$) after 2005, demonstrating the fragmentation situation of tidal vegetation. The TA of tidal flats in the LHPA first experienced a decreasing trend and then an increasing trend before 2005, and the PN showed a significantly decreasing trend ($p<.05$). However, the TA of tidal flats decreased substantially after 2005 (slope = −3.70 km^2/year, $p<.01$), and the PN had two phases: (1) a rapidly increasing phase during 2006–2013 ($p<.05$); and (2) a sharply decreasing phase during 2014–2020 ($p>.05$). In general, the LHPA was effective in halting the decreasing trends in saltmarsh and tidal flat areas after the Ramsar year, and it still had more room for enhancing the efficiency of its recovery.

The TA and PN of tidal vegetation in the Yellow River Delta National Nature Reserve-Yellow River Estuary (YRPA) experienced a substantial decrease before 2013 with rates of −3.44 km^2/year ($p<.001$) and −22.73/year ($p<.01$), respectively. After the Ramsar year, the TA of tidal vegetation in the YRPA started to increase slightly, nevertheless, its PN experienced a slight decrease. Unlike the tidal vegetation, the TA of tidal flats showed a relatively stable trend before 2013 while the PN decreased substantially ($p<.05$). After 2013, the TA and PN had two phases: (1) a significantly decreasing phase of TA and slightly increasing phases of PN during 2014–2018; and (2) an increasing phase of TA and decreasing phases of PN after 2018. Thus, the YRPA was more effective in saving and protecting saltmarshes than tidal flats after the Ramsar year.

The TA of tidal vegetation in the Shanghai Chongming Dongtan Bird National Nature Reserve (CMPA) continually increased (slope = 1.68 km^2/year, $p<.0001$) before 2005; however, the PN had two phases: a substantially increasing phase ($p<.01$) during 1984–1997; and a slightly decreasing phase during 1998–2005. After the Ramsar year, the TA of tidal vegetation continually increased during 2005–2013, but rapidly decreased during 2013–2014, and slightly increased after 2014. The PN continually increased during 2006–2020 except for the very large values in 2014. As for the tidal flats, their TA had an increasing trend over years (slope = 0.53 km^2/year, $p<.0001$), and their PN also had a non-significantly increasing trend during 1984–2020 ($p>.05$), however, the variation of PN before 2005 was much larger than that after 2005.

The TA of tidal vegetation in the Shanghai Jiuduansha Wetland National Nature Reserve (JDSPA) of the YtRD, which was subjected to very limited human disturbances, experienced substantial gains during 1984–2020. However, the PN of tidal vegetation had a relatively stable trend with large variation. The TA of tidal flats had a significantly increasing trend before 2005 (slope = 1.04 km^2/year, $p<.0001$), then it had a slightly decreasing trend after 2005 ($p>.05$). The PN of tidal flats had similar dynamics to TA before and after the NNR year. Thus, both the CMPA and JDSPA were effective in holding the increasing trends in saltmarshes and tidal flats after the NNR and Ramsar years.

4 | DISCUSSION

4.1 | Coastal wetland structure in China's four major river deltas

Due to the great importance and vulnerability of coastal wetlands in large river deltas, the dynamic analysis of coastal wetland structure (e.g., patch size and number) are becoming a research hotspot (Bianchi & Allison, 2009; Gaglio et al., 2017; Richards & Friess, 2016; Ryu et al., 2021; Webb et al., 2014), especially in China's four major river deltas, where coastal wetlands have experienced substantial changes under the pressure of intensified human activities and climate change (Li et al., 2011; Liu et al., 2014; Tan et al., 2022; Xiao & Li, 2004; Zhou et al., 2019). In this study, we used a pixel- and phenology-based mapping tool, which has been validated at multiple scales in China (Liu et al., 2020, 2023; Wang, Xiao, Zou, Chen, et al., 2020; Wang, Xiao, Zou, Hou, et al., 2020), to generate the annual maps of coastal wetlands in China's four major river deltas, and analyzed the dynamics of their patch sizes and numbers during 1984–2020. Furthermore, we also investigated the effectiveness of four PAs for saving and protecting coastal wetlands over the last three decades.

Other researchers also have completed the analysis in China's river deltas. For example, Liu et al. (2014) analyzed the spatial–temporal dynamics of wetland landscape patterns in the YRD based on remotely sensed imageries in 2000, 2005, and 2010. They found that the TA of natural coastal wetlands decreased from 2000 to 2010, which was also supported by our study. Furthermore, they found the wetland patches, which included natural and constructed wetlands, gradually became more fragmentated, complex, and decentralized in the YRD. However, our study focused on the natural tidal flats and saltmarshes separately and found their decreased PD values and less fragmented trends during 2000–2010 because of the considerable losses of coastal wetland areas (Figure 3). Zhou et al. (2019) generated maps of natural coastal wetlands and constructed wetlands of the PRD in 1980, 1990, 2000, 2010, and 2015, and found that the natural wetlands had shrunk with a TA of 189 km^2. In addition, compared with the situation in 1980, the PN of wetlands was much higher in 2015. However, in our study, we found an increased TA and PN of tidal vegetation and a slightly decreased TA of tidal flats in the PRD during 1984–2015.

Several reasons may explain the inconsistency between these published studies and our study. First, in terms of input image data,

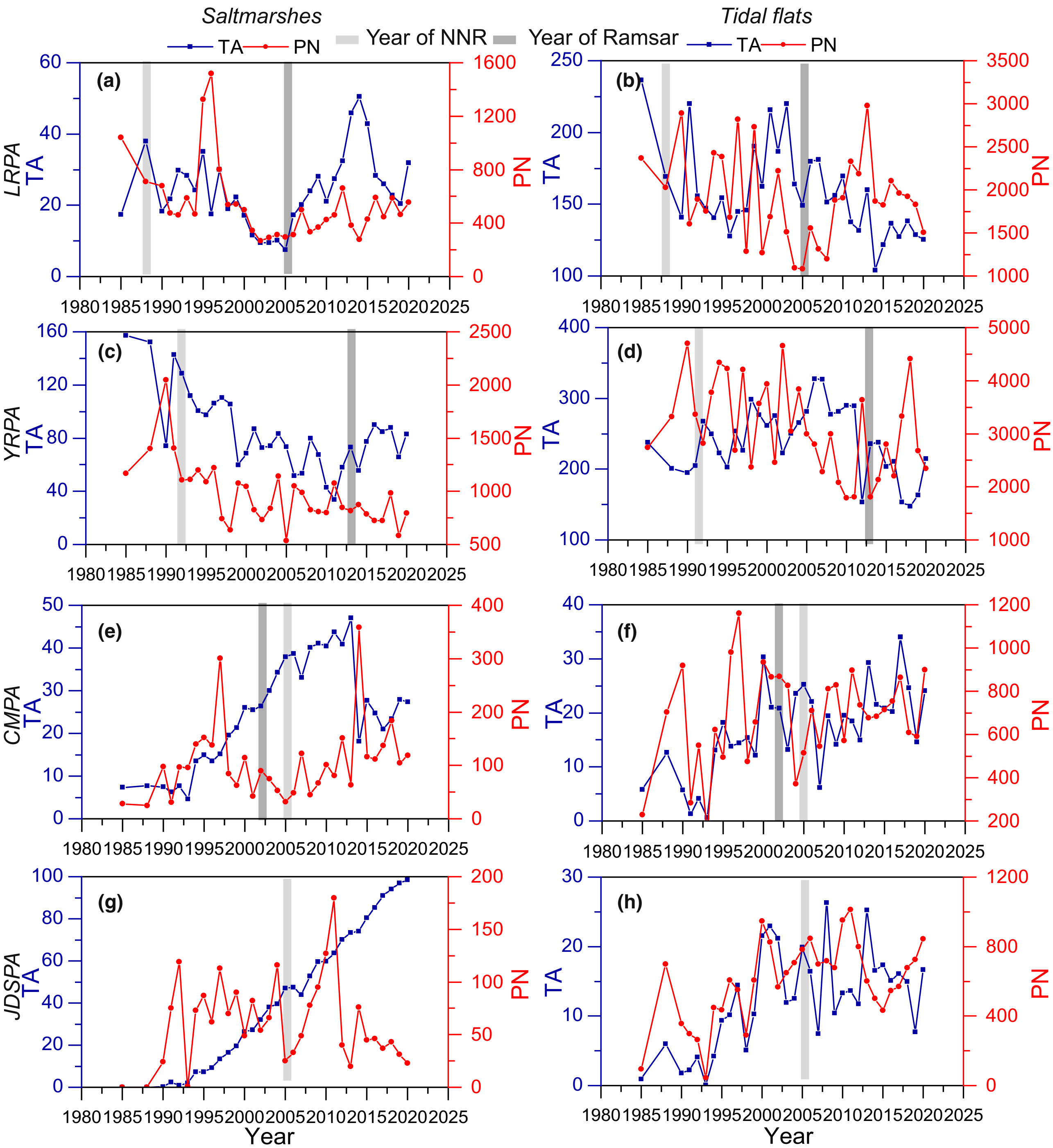

FIGURE 6 Total areas (TA, km^2) and patch numbers (PN) of saltmarshes and tidal flats in four protected areas (PAs) in China's four major river deltas during 1984–2020. (a–b) TA and PN in the LRPA. (c–d) TA and PN in the YRPA. (e–f) TA and PN in the CMPA. (g–h) TA and PN in the JDSPA. Year of NNR: The year in which PA was established as a National Nature Reserve (NNR); Year of Ramsar: The year in which PA was listed as a Ramsar site.

these studies used only one Landsat imagery from a single date or mosaicked image from multiple dates within the study region, however, our study used all the available time-series Landsat data in each year. The larger numbers of good-quality observations used in our study could provide more information on coastal wetlands, and might have obtained a more accurate estimate of coastal wetland area in our study. Second, in terms of the mapping algorithm, these published studies used either a visual interpretation method or object-oriented classification approach while we used a pixel- and phenology-based algorithm, which could reduce the effects of bad-quality observations, phenological information of tidal vegetation, and periodical tides on the identification of coastal wetlands and greatly improve the accuracy of resultant analysis (Chen et al., 2017; Wang et al., 2021). Third, in terms of land cover classification scheme and definition, these previous studies mapped all the natural and constructed coastal wetlands, but we only identified the natural coastal wetlands (including tidal flats, saltmarshes, and mangrove forests). The different definitions of study area might also have led to the different dynamics of coastal wetlands. In addition, almost all these published studies only reported the landscape dynamics of coastal wetlands in specific years before 2015, however, our study generated annual maps of coastal wetlands and extended the study period to the year 2020 from 1980s and found the divergent dynamics of patch sizes and numbers of coastal wetlands in four deltas after 2015. To our best knowledge, this is the first study that evaluated annual spatial–temporal dynamics of patch size and number in China's four large river deltas during 1984–2020.

With regards to the effectiveness of major PAs, Mao et al. (2021) have explored the wetland dynamics in China's Ramsar sites and revealed that Ramsar sites play important roles in preventing wetland loss, in comparison to the dramatic decline of wetlands in the surrounding areas. Furthermore, they have also highlighted the expansion of invasive *Spartina* in several coastal areas, especially in the coastal PAs, for example, YRPA and CMPA. In addition, Ren et al. (2021) have also analyzed the effectiveness of coastal wetland PAs and found that PAs were successful in rescuing iconic wetlands and critical shorebird habitats from once widespread reclamation, but this success was counteracted by extensive plant invasions. In our study, similar conclusions were also drawn, that is, PAs were effective in controlling the expansion of reclaimed areas but plant invasions threatened the success of PAs. Furthermore, our study also reported varying effectiveness of PAs in China's four major river deltas in halting the decreasing trends in coastal wetland areas after these PAs were listed as Ramsar Sites through analyzing the annual dynamics of TA and PN of coastal wetlands.

4.2 | Anthropogenic drivers for coastal wetland dynamics

Coastal reclamation, the process of creating new land from the sea, is regarded as one of the most important factors that are driving the rapid changes of coastal wetlands, and leads to reduced biodiversity, worse water quality, reduced ability of carbon storage and coastal protection from storm events, and increased regional vulnerability to sea level rise (Cheng et al., 2020; Jiang et al., 2021; Ma et al., 2014). In this study, we found that China's four major river deltas experienced drastic reclamations since the 1980s, resulting in the substantial losses of coastal wetlands in the LRD and YRD. For example, the reclamation activities in the LRD and LHPA resulted in the substantial decrease in the saltmarsh areas (Figure S11). To protect the environment and maintain the sustainability of coastal wetlands, China's government has implemented several environmental laws and regulations since the 1980s (Hua, 2014; Jiang et al., 2021; Li et al., 2020; Wang et al., 2014), such as the release of the Notice on Issues related to Intensifying Management of Land Reclamation Plans in 2010 and Procedure for Management of Land Reclamation Plans in 2011, both of which aim to specify the detailed procedure of making, implementing, and supervising annual reclamation quota plans (Jiang et al., 2021), as well as the approval of National Marine Function Zoning Plan (2011–2020) in 2012, which aims to strengthen the management of reclamation projects and to rationally control the scale of reclamation (Ma et al., 2014). All these measures have slowed down the reclamation, and our study also provided strong evidence that the reclaimed areas in four deltas decreased substantially over the last few years (Figure S6d–g). The decreased reclaimed areas in four deltas have great contribution to the recent recovery of tidal vegetation and tidal flats (Wang et al., 2021), such as the recent recovery of saltmarshes in the LRD and YtRD, as well as the continually increased area of tidal vegetation in the PRD (Figure 3).

Large-scale dams have been constructed in China's large rivers to meet the growing needs for water resources required for an increasing population and controlling of seasonal flooding (Yang & Lu, 2014). One example is the Three Gorges Dam (TGD) in the Yangtze River of western Hubei Province, the largest hydroelectric dam in the world, which contributes to the substantial decrease of sediment discharge in the Yangtze River (Figure S12a). The TGD reservoir was first impounded in 2003, then the water level increased to 175 m (the maximum height by dam design) in October 2010 (Wang et al., 2013, 2014). During 2003–2010, the low and decreased sediment load, as well as the large and increased reclaimed areas, contributed to the substantial losses of saltmarsh and tidal flat areas and increased PNs in the YtRD (Figure S12a,b). Furthermore, our findings highlight that the reclaimed areas have larger effects on the PN dynamics of saltmarshes than sediment discharge in these years (Figure S13). After 2012, the reclaimed areas decreased and stayed at a very low level by 2020, contributing to the recent recovery of saltmarsh and tidal flats in all four deltas.

In addition to the reclamation and sediment discharge, ecological restoration projects in the coastal zone also have great impacts on the dynamics of coastal wetlands (Jia et al., 2021; Liu et al., 2014; Zhang, Xiao, et al., 2020), such as the Ecological Engineering Project of Controlling *Spartina* (US$ 186 million, hereafter, EEPCS) implemented during 2013–2016 in CMPA of the YtRD (Figure S14), which contained three major components: eradiation of invasive *Spartina*, restoration of native plant saltmarsh communities, and reconstruction of bird habitats (Zhang, Xiao, et al., 2020). EEPCS caused substantial decreases of PN and TA of medium- to large-size saltmarshes (area ≥0.01 km^2) and increased the TA of tidal flats in CMPA during 2013–2016 due to the removal of *Spartina* in the first step (Figure S12c,d), after which the PN and TA of saltmarshes started to increase and the PN of tidal flats started to decrease at high rates due to the restoration of native plant (e.g., *Scirpus* × *mariqueter*) saltmarshes (Zhang, Xiao, et al., 2020). Although the restoration project has contributed to the losses of invasive *Spartina* and the gains of native saltmarsh plants, this project covered a very limited range, and the conservation of saltmarsh ecosystems still lags far behind the invasion of

Spartina (Jackson et al., 2021; Mao et al., 2019; Wang et al., 2022). Considering the important ecosystem services of native saltmarshes, there is an urgent need to put more effort into the protection and restoration of native saltmarshes at a much larger scale.

4.3 | Impact of plant invasions on coastal wetland dynamics

Plant invasions are one of the most important interventions on the dynamics of coastal wetlands in China's coastal zone, especially *Spartina*, which has the great invading ability, and has well established in the intertidal zones and become the most dominant species in saltmarshes in China (Ning et al., 2021; Wang et al., 2022; Zhang, Xiao, et al., 2020). Since the 1980s, the areas of *Spartina* saltmarshes continually increased in China's coastal zone as they expanded rapidly from 0.001 km^2 in 1981 to approximately 520 km^2 in 2020 (Li et al., 2022), especially in large river deltas, as the proportions of the total saltmarsh areas have raised to ~20% in the YRD and ~28% in the YtRD in 2020, and the proportions of their PN accounted for ~40% in the YRD and ~55% in the YtRD in 2020 (Figure S15). As *Spartina* saltmarshes could alter the estuarine sediment dynamics and outcompete native plant species, the expansion of *Spartina* usually decreases the PNs of total saltmarsh and contributed to the smaller fragmentation (Liu et al., 2018). Our study also supported that the *Spartina* saltmarsh area in JDSPA, which has very limited human disturbances, increased substantially since 2000 (Figure S16a), and the expanded *Spartina* saltmarshes had a significant contribution to the decreased PNs of saltmarshes (Figure S16b).

However, the rapid and extensive spread of *Spartina* saltmarshes has threatened coastal sustainable environments through out-competing native plant species, preventing water birds from obtaining food from mudflats, and reducing coastal biodiversity (Li et al., 2022; Wang et al., 2022). As the target of the "no net loss" policy measures total changes without considering changes in composition and the corresponding ecological functions (He, 2019; Mao et al., 2022; Xu et al., 2019), the *Spartina*-induced no net loss of coastal wetlands in patch sizes and numbers do not really represent the real improvement of wetland quality, functions, biodiversity, and ecosystem services. Thus, given its rapid expansion and notable negative ecological consequences, it is necessary to monitor the *Spartina* invasions in the saltmarshes for the sake of scientific ecosystem management and conservation, and replace them with native saltmarshes for the conservation and restoration of coastal wetlands in China (Mao et al., 2019; Wang et al., 2021). Furthermore, the effects of rapidly expanding *Spartina* on the ecosystem structure and functioning (such as soil carbon sequestration) of natural wetlands are still unclear, which calls for comprehensive research on the effects of plant invasions, the functions of coastal wetlands, and how to restore their functions (He, 2019).

TABLE 1 Reclamation and *Spartina* areas (km^2) in four protected areas (PAs) of China's major river deltas before and after Ramsar years

	Reclaimed area		*Spartina* area	
PAs	Before	After	Before	After
LHPA	148.58	70.01	0.02	0.48
YRPA	139.57	20.64	3.67	85.58
CMPA	0.82	23.74	0.53	78.68
JDSPA	—	—	7.41	352.07

Note: "—" means there is no reclamation in JDSPA. Note that JDSPA has not been listed as a Ramsar site, and here we calculated the areas before and after the year in which JDSPA was established as National Nature Reserve.

4.4 | Effectiveness of PAs for protecting biodiversity in four deltas

Protected areas, which have more than tripled in number and size globally, have effectively conserved habitats and biodiversity against losses driven by human activities (Mao et al., 2021; Ren et al., 2021). In China's four major river deltas, four PAs have been established as NNRs, three of which have been listed as Ramsar sites (Table S1), and are playing critical roles in halting the decreasing trends in coastal wetland areas (Ren et al., 2021). Our findings also supported that the tidal vegetation and tidal flat areas in these PAs had stable or increasing trends after the establishment (Figure 6). In addition, we also found that the reclaimed areas have recently experienced significant decreases in these PAs (Figure S17). In particular, reclaimed areas of these PAs became much smaller after they were listed as Ramsar sites except for that of the CMPA because of the EEPCS (Table 1), indicating the strong effectiveness of PAs in controlling the expansion of reclaimed areas.

However, the success of PAs in preventing the expansion of reclamation is being threatened by extensive plant invasions. From the long-term analysis, our study found that the areas invaded by *Spartina* increased substantially in the four PAs (Figure S17). Furthermore, the *Spartina*-invaded areas in four PAs were much larger after Ramsar sites were designated (Table 1). The expansion of *Spartina* saltmarshes not only affects the patch size and number of coastal wetlands but also has great negative effects on the succession of new native marshes and the protection of water birds and biodiversity (Li et al., 2022; Wang et al., 2022). Our findings have important implications for understanding the information on effectiveness of PAs in stopping land reclamation and expansion of plant invasions in China's major river deltas. In addition, our findings also suggest that it is urgent to control the reclamation and plant invasions to safeguard PAs as effective refugia for highly valued coastal wetland ecosystems and biodiversity and maintain the sustainability of coastal wetlands in China.

In addition, the PAs had different effectiveness in protecting different types of coastal wetlands. Considering the important ecosystem services of saltmarsh ecosystems, many conservation efforts in PAs have led to the recovery of saltmarshes, such as the restoration project in the YRPA (Zhou et al., 2016) and the restoration of native *Scirpus × mariqueter* saltmarshes in the CMPA (Zhang, Qiu, et al., 2020). However, few conservation and restoration plans in PAs have been introduced for tidal flats, which spread across 18,000 km of China's coastline and cover the largest areas in the coastal zone serving as critical wildlife habitats for many species of waterfowl and migratory birds (Jia et al., 2021). Our study also found that PAs in China's major river deltas had stronger effectiveness in saving and protecting saltmarshes than tidal flats (Figure 6). Thus, to maintain the sustainability of coastal wetlands in PAs, more efforts are needed to protect tidal flats by establishing new protection laws and regulations, and by increasing financial support for tidal flat research.

4.5 | Uncertainties of the analysis of coastal wetland structure

Our study analyzed the divergent dynamics of coastal wetland structure (patch size and number) in China's four large river deltas by producing detailed and accurate maps of coastal wetlands (tidal flats, saltmarshes, and mangrove forests), and investigated the impacts of reclamation, dam construction, ecological engineering projects, plant invasions, and the effectiveness of PAs. Our study, together with previously published studies (Li et al., 2011; Liu et al., 2014; Tan et al., 2022), contributed to our knowledge about the coastal wetland structure and coastal sustainability in China's major river deltas. However, we must also recognize the potential sources of errors and uncertainties in our analysis. First, as the spatial resolution of Landsat imagery is 30 m, those small patches of coastal wetlands with areas $<30 \times 30\,m^2$ could not be mapped in our study. Second, the Landsat image quality might have affected the analysis in our study. For example, the number of images of China's coastal provinces was much lower in 2012 than in other years (Figure S1), which appeared to lead to the low coastal wetland areas recorded in 2012 in some deltas, such as the very low tidal flat area in the YtRD in 2012 (Figure 3g). Third, our study reported the structure of three major coastal wetland types, of which saltmarshes have many communities that are dominated respectively by *Tamarix chinensis*, *Phragmites australis*, *Suaeda salsa*, *Scirpus mariqueter*, *Cyperus malaccensis*. In the future, we could further explore the fine classification of saltmarshes and mangroves by dominant species, and investigate their structural dynamics under natural or anthropogenic disturbances.

5 | CONCLUSION

Our satellite-based analysis reveals rapid and large changes in coastal wetland structure (patch size and number) in China's four major river deltas. Both TA and PN in the LRD and YRD experienced substantial losses over the last three decades, and they had a non-significantly but recently increasing trend in the YtRD. The PRD showed a relatively stable but variable trend in TA but a continually increasing trend in PN. Furthermore, the tidal vegetation and tidal flats had divergent dynamics in their TA and PN due to coastal reclamation, reduced sediment loads in the rivers, expansion of invasive plants, and ecological restoration projects. We also found that PAs were effective in halting the decreasing trends in saltmarsh and tidal flat areas, but still, there are great potentials to be improved, especially, the success of PAs in slowing the expansion of reclamation is being counteracted by soaring exotic plant invasions. Our study provides vital information for the government, stakeholders, and the public to address increasing challenges of coastal management, restoration, and sustainability in large river deltas.

ACKNOWLEDGMENTS

This study was supported by the National Key Research and Development Program of China (2022YFC2601100), the Natural Science Foundation of China (32030067, 42201341, and 41630528), the China Postdoctoral Science Foundation (2021TQ0072 and 2021M700835), and the US National Science Foundation (1911955 and 2200310).

CONFLICT OF INTEREST

The authors declare no conflict of interest.

DATA AVAILABILITY STATEMENT

Current Landsat Collection 2 Level-2 (TM/ETM/OLI) surface reflectance (SR) data are available through the Google Earth Engine cloud-processing platform (Landsat 8: https://developers.google.com/earth-engine/datasets/catalog/LANDSAT_LC08_C02_T1_L2; Landsat 7: https://developers.google.com/earth-engine/datasets/catalog/LANDSAT_LE07_C02_T1_L2; Landsat 5: https://developers.google.com/earth-engine/datasets/catalog/LANDSAT_LT05_C02_T1_L2). Annual sea level anomaly data during 1984-2020 in China were collected from the China Sea Level Bulletin (http://www.mnr.gov.cn/sj/sjfw/hy/gbgg/zghpmgb/). Annual sediment load data in the four deltas for the period 1984-2020 were collected from the annual Chinese River Sediment Bulletin (http://www.irtces.org/nszx/cbw/hlnsgb/A550406index_1.htm). The Google Earth Engine code for identifying coastal wetlands and *Spartina* saltmarsh are from Wang et al. (2021) and Zhang, Xiao, et al. (2020). The classified coastal weltand maps in China's four major river deltas are available on Figshare at https://doi.org/10.6084/m9.figshare.21819690.v1.

ORCID

Xinxin Wang https://orcid.org/0000-0001-8013-3660
Xiangming Xiao https://orcid.org/0000-0003-0956-7428
Xi Zhang https://orcid.org/0000-0001-8515-6941
Jihua Wu https://orcid.org/0000-0001-8623-8519
Bo Li https://orcid.org/0000-0002-0439-5666

REFERENCES

Barbier, E. B., Hacker, S. D., Kennedy, C., Koch, E. W., Stier, A. C., & Silliman, B. R. (2011). The value of estuarine and coastal ecosystem services. *Ecological Monographs*, *81*(2), 169–193. https://doi.org/10.1890/10-1510.1

Bianchi, T. S., & Allison, M. A. (2009). Large-river delta-front estuaries as natural "recorders" of global environmental change. *Proceedings of the National Academy of Sciences of the United States of America*, *106*(20), 8085–8092. https://doi.org/10.1073/pnas.0812878106

Chen, B. Q., Xiao, X. M., Li, X. P., Pan, L. H., Doughty, R., Ma, J., Dong, J. W., Qin, Y. W., Zhao, B., Wu, Z. X., Sun, R., Lan, G. Y., Xie, G. S., Clinton, N., & Giri, C. (2017). A mangrove forest map of China in 2015: Analysis of time series Landsat 7/8 and sentinel-1A imagery in Google Earth Engine cloud computing platform. *ISPRS Journal of Photogrammetry and Remote Sensing*, *131*, 104–120. https://doi.org/10.1016/j.isprsjprs.2017.07.011

Chen, Y., Dong, J. W., Xiao, X. M., Ma, Z. J., Tan, K., Melville, D., Li, B., Lu, H. Y., Liu, J. F., & Liu, F. S. (2019). Effects of reclamation and natural changes on coastal wetlands bordering China's Yellow Sea from 1984 to 2015. *Land Degradation & Development*, *30*(13), 1533–1544. https://doi.org/10.1002/ldr.3322

Cheng, Z., Jalon-Rójas, I., Wang, X. H., & Liu, Y. (2020). Impacts of land reclamation on sediment transport and sedimentary environment in a macro-tidal estuary. *Estuarine, Coastal and Shelf Science*, *242*, 106861. https://doi.org/10.1016/j.ecss.2020.106861

Croxall, J. P., Butchart, S. H. M., Lascelles, B., Stattersfield, A. J., Sullivan, B., Symes, A., & Taylor, P. (2012). Seabird conservation status, threats and priority actions: A global assessment. *Bird Conservation International*, *22*(1), 1–34. https://doi.org/10.1017/S0959270912000020

Gaglio, M., Aschonitis, V. G., Gissi, E., Castaldelli, G., & Fano, E. A. (2017). Land use change effects on ecosystem services of river deltas and coastal wetlands: Case study in Volano–Mesola–Goro in Po river delta (Italy). *Wetlands Ecology and Management*, *25*(1), 67–86. https://doi.org/10.1007/s11273-016-9503-1

Haddad, N. M., Brudvig, L. A., Clobert, J., Davies, K. F., Gonzalez, A., Holt, R. D., Lovejoy, T. E., Sexton, J. O., Austin, M. P., Collins, C. D., Cook, W. M., Damschen, E. I., Ewers, R. M., Foster, B. L., Jenkins, C. N., King, A. J., Laurance, W. F., Levey, D. J., Margules, C. R., … Townshend, J. R. (2015). Habitat fragmentation and its lasting impact on Earth's ecosystems. *Science Advances*, *1*(2), 1–10. https://doi.org/10.1126/sciadv.1500052

He, Q. (2019). Conservation: 'No net loss' of wetland quantity and quality. *Current Biology*, *29*(20), R1070–R1072. https://doi.org/10.1016/j.cub.2019.08.027

He, Q., & Silliman, B. R. (2019). Climate change, human impacts, and coastal ecosystems in the Anthropocene. *Current Biology*, *29*(19), R1021–R1035. https://doi.org/10.1016/j.cub.2019.08.042

Hua, Y. (2014). Legal regulation of land reclamation in China's coastal areas. *Coastal Management*, *42*(1), 59–79. https://doi.org/10.1080/08920753.2013.865008

Jackson, M. V., Fuller, R. A., Gan, X., Li, J., Mao, D., Melville, D. S., Murray, N. J., Wang, Z., & Choi, C. Y. (2021). Dual threat of tidal flat loss and invasive *Spartina alterniflora* endanger important shorebird habitat in coastal mainland China. *Journal of Environmental Management*, *278*, 111549. https://doi.org/10.1016/j.jenvman.2020.111549

Jia, M., Wang, Z., Mao, D., Ren, C., Wang, C., & Wang, Y. (2021). Rapid, robust, and automated mapping of tidal flats in China using time series Sentinel-2 images and Google earth engine. *Remote Sensing of Environment*, *255*, 112285. https://doi.org/10.1016/j.rse.2021.112285

Jiang, S., Xu, N., Li, Z., & Huang, C. (2021). Satellite derived coastal reclamation expansion in China since the 21st century. *Global Ecology and Conservation*, *30*, e01797. https://doi.org/10.1016/j.gecco.2021.e01797

Li, F., Ding, D., Chen, Z., Chen, H., Shen, T., Wu, Q., & Zhang, C. (2020). Change of sea reclamation and the sea-use management policy system in China. *Marine Policy*, *115*, 103861. https://doi.org/10.1016/j.marpol.2020.103861

Li, H., Mao, D., Wang, Z., Huang, X., Li, L., & Jia, M. (2022). Invasion of *Spartina alterniflora* in the coastal zone of mainland China: Control achievements from 2015 to 2020 towards the sustainable development goals. *Journal of Environmental Management*, *323*, 116242. https://doi.org/10.1016/j.jenvman.2022.116242

Li, J., Wang, A. J., & Li, T. J. (2011). Variations of coastal wetland landscapes in the Pearl River Delta in the last 20 years. *Advances in Marine Science*, *2*, 170–178.

Lindenmayer, D. (2019). Small patches make critical contributions to biodiversity conservation. *Proceedings of the National Academy of Sciences of the United States of America*, *116*(3), 717–719. pnas.1820169116

Liu, G. L., Zhang, L. C., Zhang, Q., Musyimi, Z., & Jiang, Q. H. (2014). Spatio-temporal dynamics of wetland landscape patterns based on remote sensing in Yellow River Delta, China. *Wetlands*, *34*(4), 787–801. https://doi.org/10.1007/s13157-014-0542-1

Liu, M., Mao, D., Wang, Z., Li, L., Man, W., Jia, M., Ren, C., & Zhang, Y. (2018). Rapid invasion of *Spartina alterniflora* in the coastal zone of mainland China: New observations from Landsat OLI images. *Remote Sensing*, *10*, 1933. https://doi.org/10.3390/rs10121933

Liu, Y., Li, J., Sun, C., Wang, X., Tian, P., Chen, L., Zhang, H., Yang, X., & He, G. (2023). Thirty-year changes of the coastlines, wetlands, and ecosystem services in the Asia major deltas. *Journal of Environmental Management*, *326*, 116675. https://doi.org/10.1016/j.jenvman.2022.116675

Liu, Y.-F., Ma, J., Wang, X.-X., Zhong, Q.-Y., Zong, J.-M., Wu, W.-B., Wang, Q., & Zhao, B. (2020). Joint effect of *Spartina alterniflora* invasion and reclamation on the spatial and temporal dynamics of tidal flats in Yangtze River estuary. *Remote Sensing*, *12*(11), 1725. https://doi.org/10.3390/rs12111725

Ma, T. T., Li, X. W., Bai, J. H., & Cui, B. S. (2019). Tracking three decades of land use and land cover transformation trajectories in China's large river deltas. *Land Degradation & Development*, *30*(7), 799–810. https://doi.org/10.1002/ldr.3268

Ma, Z., Melville, D. S., Liu, J., Chen, Y., Yang, H., Ren, W., Zhang, Z., Piersma, T., & Li, B. (2014). Rethinking China's new great wall. *Science*, *346*(6212), 912–914. https://doi.org/10.1126/science.1257258

Mao, D., Liu, M., Wang, Z., Li, L., Man, W., Jia, M., & Zhang, Y. (2019). Rapid invasion of *Spartina alterniflora* in the coastal zone of mainland China: Spatiotemporal patterns and human prevention. *Sensors*, *19*(10), 2308. https://doi.org/10.3390/s19102308

Mao, D., Wang, Z., Wang, Y., Choi, C.-Y., Jia, M., Jackson, M. V., & Fuller, R. A. (2021). Remote observations in China's Ramsar sites: Wetland dynamics, anthropogenic threats, and implications for sustainable development goals. *Journal of Remote Sensing*, *2021*, 9849343. https://doi.org/10.34133/2021/9849343

Mao, D., Yang, H., Wang, Z., Song, K., Thompson, J. R., & Flower, R. J. (2022). Reverse the hidden loss of China's wetlands. *Science*, *376*(6597), 1061. https://doi.org/10.1126/science.adc8833

Murray, N. J., Worthington, T. A., Bunting, P., Duce, S., Hagger, V., Lovelock, C. E., Lucas, R., Saunders, M. I., Sheaves, M., Spalding, M., Waltham, N. J., & Lyons, M. B. (2022). High-resolution mapping of losses and gains of Earth's tidal wetlands. *Science*, *376*(6594), 744–749. https://doi.org/10.1126/science.abm9583

Ning, Z., Chen, C., Xie, T., Wang, Q., Bai, J., Shao, D., Man, Y., & Cui, B. (2020). Windows of opportunity for smooth cordgrass landward invasion to tidal channel margins: The importance of hydrodynamic disturbance to seedling establishment. *Journal of Environmental*

Management, *266*, 110559. https://doi.org/10.1016/j.jenvman.2020.110559
Ning, Z., Chen, C., Xie, T., Zhu, Z., Wang, Q., Cui, B., & Bai, J. (2021). Can the native faunal communities be restored from removal of invasive plants in coastal ecosystems? A global meta-analysis. *Global Change Biology*, *27*(19), 4644–4656. https://doi.org/10.1111/gcb.15765
Ning, Z., Xie, T., Liu, Z., Bai, J., & Cui, B. (2019). Native herbivores enhance the resistance of an anthropogenically disturbed salt marsh to *Spartina alterniflora* invasion. *Ecosphere*, *10*(1), e02565. https://doi.org/10.1002/ecs2.2565
R Core Team. (2021). *R: A language and environment for statistical computing*. R Foundation for Statistical Computing. https://www.r-project.org/
Ren, J., Chen, J., Xu, C., van de Koppel, J., Thomsen, M. S., Qiu, S., Cheng, F., Song, W., Liu, Q. X., Xu, C., Bai, J., Zhang, Y., Cui, B., Bertness, M. D., Silliman, B. R., Li, B., & He, Q. (2021). An invasive species erodes the performance of coastal wetland protected areas. *Science Advances*, *7*(42), eabi8943. https://doi.org/10.1126/sciadv.abi8943
Richards, D. R., & Friess, D. A. (2016). Rates and drivers of mangrove deforestation in Southeast Asia, 2000-2012. *Proceedings of the National Academy of Sciences of the United States of America*, *113*(2), 344–349. https://doi.org/10.1073/pnas.1510272113
Ryu, J., Liu, K. B., Bianchette, T. A., & McCloskey, T. (2021). Identifying forcing agents of environmental change and ecological response on the Mississippi River Delta, southeastern Louisiana. *Science of the Total Environment*, *794*, 148730. https://doi.org/10.1016/j.scitotenv.2021.148730
Tan, Y., Yang, Q., Jia, M., Xi, Z., Wang, Z., & Mao, D. (2022). Remote sensing monitoring and analysis of the impact of human activities on wetland in Liaohe estuary National Nature Reserve. *Remote Sensing Technology and Application*, *37*(1), 218–230. https://doi.org/10.11873/j.issn.1004-0323.2022.1.0218
Timmers, R., van Kuijk, M., Verweij, P. A., Ghazoul, J., Hautier, Y., Laurance, W. F., Arriaga-Weiss, S. L., Askins, R. A., Battisti, C., Berg, Å., Daily, G. C., Estades, C. F., Frank, B., Kurosawa, R., Pojar, R. A., Woinarski, J. C. Z., & Soons, M. B. (2022). Conservation of birds in fragmented landscapes requires protected areas. *Frontiers in Ecology and the Environment*, *20*(6), 361–369. https://doi.org/10.1002/fee.2485
Wang, J., Sheng, Y., Gleason, C. J., & Wada, Y. (2013). Downstream Yangtze River levels impacted by Three Gorges Dam. *Environmental Research Letters*, *8*(4), 044012. https://doi.org/10.1088/1748-9326/8/4/044012
Wang, J., Sheng, Y., & Tong, T. S. D. (2014). Monitoring decadal lake dynamics across the Yangtze Basin downstream of Three Gorges Dam. *Remote Sensing of Environment*, *152*, 251–269. https://doi.org/10.1016/j.rse.2014.06.004
Wang, X., Xiao, X., He, Q., Zhang, X., Wu, J., & Li, B. (2022). Biological invasions in China's coastal zone. *Science*, *378*(6623), 957. https://doi.org/10.1126/science.ade9665
Wang, X., Xiao, X., Xu, X., Zou, Z., Chen, B., Qin, Y., Zhang, X., Dong, J., Liu, D., Pan, L., & Li, B. (2021). Rebound in China's coastal wetlands following conservation and restoration. *Nature Sustainability*, *4*, 1076–1083. https://doi.org/10.1038/s41893-021-00793-5
Wang, X., Xiao, X., Zou, Z., Chen, B., Ma, J., Dong, J., Doughty, R. B., Zhong, Q., Qin, Y., Dai, S., Li, X., Zhao, B., & Li, B. (2020). Tracking annual changes of coastal tidal flats in China during 1986–2016 through analyses of Landsat images with Google earth engine. *Remote Sensing of Environment*, *238*(1), 110987. https://doi.org/10.1016/j.rse.2018.11.030
Wang, X., Xiao, X., Zou, Z., Hou, L., Qin, Y., Dong, J., Doughty, R. B., Chen, B., Zhang, X., Chen, Y., Ma, J., Zhao, B., & Li, B. (2020). Mapping coastal wetlands of China using time series Landsat images in 2018 and Google earth engine. *ISPRS Journal of Photogrammetry and Remote Sensing*, *163*, 312–326. https://doi.org/10.1016/j.isprsjprs.2020.03.014
Webb, E. L., Jachowski, N. R. A., Phelps, J., Friess, D. A., Than, M. M., & Ziegler, A. D. (2014). Deforestation in the Ayeyarwady Delta and the conservation implications of an internationally-engaged Myanmar. *Global Environmental Change*, *24*(1), 321–333. https://doi.org/10.1016/j.gloenvcha.2013.10.007
Wilson, M. C., Chen, X. Y., Corlett, R. T., Didham, R. K., Ding, P., Holt, R. D., Holyoak, M., Hu, G., Hughes, A. C., Jiang, L., Laurance, W. F., Liu, J., Pimm, S. L., Robinson, S. K., Russo, S. E., Si, X., Wilcove, D. S., Wu, J., & Yu, M. (2016). Habitat fragmentation and biodiversity conservation: Key findings and future challenges. *Landscape Ecology*, *31*(2), 219–227. https://doi.org/10.1007/s10980-015-0312-3
Xiao, D. N., & Li, X. Z. (2004). Ecological and environmental function of wetland landscape in the Liaohe Delta. In M. H. Wong (Ed.), *Wetlands ecosystems in Asia* (Vol. *1*, pp. 35–46). Elsevier. https://doi.org/10.1016/B978-044451691-6/50006-5
Xie, C., Cui, B., Xie, T., Yu, S., Liu, Z., Chen, C., Ning, Z., Wang, Q., Zou, Y., & Shao, X. (2020). Hydrological connectivity dynamics of tidal flat systems impacted by severe reclamation in the Yellow River Delta. *Science of the Total Environment*, *739*, 139860. https://doi.org/10.1016/j.scitotenv.2020.139860
Xu, W., Fan, X., Ma, J., Pimm, S. L., Kong, L., Zeng, Y., Li, X., Xiao, Y., Zheng, H., Liu, J., Wu, B., An, L., Zhang, L., Wang, X., & Ouyang, Z. (2019). Hidden loss of wetlands in China. *Current Biology*, *29*(18), 3065–3071.e3062. https://doi.org/10.1016/j.cub.2019.07.053
Yang, H., Ma, M., Thompson, J. R., & Flower, R. J. (2017). Protect coastal wetlands in China to save endangered migratory birds. *Proceedings of the National Academy of Sciences of the United States of America*, *114*(28), E5491–E5492. https://doi.org/10.1073/pnas.1706111114
Yang, X., & Lu, X. (2014). Drastic change in China's lakes and reservoirs over the past decades. *Scientific Reports*, *4*, 6041. https://doi.org/10.1038/srep06041
Zhang, Q., Qiu, S., Zhu, Y., Cui, X., He, Q., & Li, B. (2020). Propagule types and environmental stresses matter in saltmarsh plant restoration. *Ecological Engineering*, *143*(15), 105693. https://doi.org/10.1016/j.ecoleng.2019.105693
Zhang, X., Xiao, X., Wang, X., Xu, X., Chen, B., Wang, J., Ma, J., Zhao, B., & Li, B. (2020). Quantifying expansion and removal of *Spartina alterniflora* on Chongming Island, China, using time series Landsat images during 1995–2018. *Remote Sensing of Environment*, *247*(15), 111916. https://doi.org/10.1016/j.rse.2020.111916
Zhou, C., Mao, Q., Xu, X., Fang, C., Luo, Y., & Li, B. (2016). Preliminary analysis of C sequestration potential of blue carbon ecosystems on Chinese coastal zone, Science China. *Life Sciences*, *46*(4), 475–486. https://doi.org/10.1360/N052016-00105
Zhou, H., Du, J., Nan, Y., Song, K., Zhao, B., & Xiang, X. (2019). Landscape patterns of coastal wetlands in Pearl River Delta and their changes for 5 periods since 1980. *Wetland Science*, *17*, 559–566. https://doi.org/10.13248/j.cnki.wetlandsci.2019.05.009
Zou, Z. H., Xiao, X. M., Dong, J. W., Qin, Y. W., Doughty, R. B., Menarguez, M. A., Zhang, G. L., & Wang, J. (2018). Divergent trends of open-surface water body area in the contiguous United States from 1984 to 2016. *Proceedings of the National Academy of Sciences of the United States of America*, *115*(15), 3810–3815. https://doi.org/10.1073/pnas.1719275115

SUPPORTING INFORMATION

Additional supporting information can be found online in the Supporting Information section at the end of this article.

How to cite this article: Wang, X., Xiao, X., Zhang, X., Wu, J., & Li, B. (2023). Rapid and large changes in coastal wetland structure in China's four major river deltas. *Global Change Biology*, *00*, 1–15. https://doi.org/10.1111/gcb.16583